Dependence of the O_2 diffusion rate on oxide thickness during silicon oxidation

2003 J. Phys.: Condens. Matter 15 S1553

(http://iopscience.iop.org/0953-8984/15/16/305)

INSTITUTE OF PHYSICS PUBLISHING JOURNAL OF PHYSICS: CONDENSED MATTER

J. Phys.: Condens. Matter **15** (2003) S1553–S1560 PII: S0953-8984(03)54800-7

Dependence of the O_2 diffusion rate on oxide thickness during silicon oxidation

Angelo Bongiorno and Alfredo Pasquarello

Institut de Théorie des Phénomènes Physiques (ITP), Ecole Polytechnique Fédérale de Lausanne (EPFL), CH-1015 Lausanne, Switzerland
and
Institut Romand de Recherche Numérique en Physique des Matériaux (IRRMA), CH-1015 Lausanne, Switzerland

E-mail: Angelo.Bongiorno@epfl.ch and Alfredo.Pasquarello@epfl.ch

Received 16 October 2002
Published 14 April 2003
Online at stacks.iop.org/JPhysCM/15/S1553

Abstract

We address the rate of O_2 diffusion through the oxide layer at Si–SiO_2 interfaces using an atomic-scale approach. In particular, we investigate the combined effect of a percolative diffusion mechanism and of a dense oxide layer located close to the silicon substrate. We first extend our atomic-scale description of O_2 diffusion in amorphous SiO_2 to the case of a densified oxide. This yields an activation energy which compares well with the experimental result. Next, we investigate the dependence of the O_2 diffusion rate on oxide thickness at Si–SiO_2 interfaces using Monte Carlo simulations. We consider both homogeneous and nonhomogeneous oxide layers. The nonhomogeneous oxide is composed of two layers, a normal and a densified one. The thickness and the mass density of the densified layer are taken from experiment. In the case of a normal oxide, we find that the O_2 diffusion rate increases with decreasing thickness, as a result of the percolative nature of the diffusion mechanism. When a densified layer is inserted, the diffusion coefficient drops below its value for bulk amorphous SiO_2, for oxide thicknesses larger than 2 nm. This result is consistent with the experimental behaviour of the oxidation kinetics.

1. Introduction

The gate dielectric in Si-based electronic devices is mostly composed of thermally grown silicon oxide layers [1]. An understanding of the oxidation mechanism leading to the formation of the oxide structure is critical for further progress in device performance. Since the seminal work of Deal and Grove [2], the most generally adopted model for silicon oxidation assumes that an oxygen species first enters the SiO_2 layer, then diffuses through the disordered oxide towards the Si–SiO_2 interface, and finally reacts at the Si substrate, where the new oxide grows. For thick oxides (>20 nm), the oxidation kinetics is dominated by the oxygen diffusion process

and is accurately accounted for by the Deal–Grove model [2]. However, in the thin-oxide-film regime, the Deal–Grove model fails to properly describe the growth kinetics [3, 4]. In fact, in this regime, the oxidation rates appear anomalously accelerated when compared to the prediction of the Deal–Grove model [3, 4]. Many interpretations have been put forward to describe this behaviour [3–5]. The best accredited among them assumes that the diffusion rate of the oxidizing species shows a spatial dependence across the oxide layer [3, 4]. As a matter of fact, this assumption is currently adopted in modern models which successfully account for the silicon oxidation kinetics in both the thin- and the thick-oxide regimes [6–8]. However, an atomic-scale description of the diffusion rate corroborating this behaviour is still lacking.

Very recently, we provided an atomic-scale description of the O_2 diffusion process in amorphous SiO_2 [9]. We used three different methodologies in sequence: first-principles calculations, classical molecular dynamics, and Monte Carlo simulations. First-principles calculations were used to provide an accurate description of the energetics of oxygen species embedded in a disordered SiO_2 network. This investigation confirmed that the interstitial O_2 molecule is the most stable oxygen species in amorphous SiO_2. We then derived classical interatomic potentials which accurately reproduced the interactions found by first-principles calculations between the O_2 molecule and the SiO_2 network. Using this classical scheme, we derived a complete picture of the potential energy landscape for O_2 diffusion in amorphous SiO_2. In particular, we found the location of energy minima and saddle points, as well as the distributions of their energies. These results confirmed the picture that the interstitial O_2 molecule is the migrating species in amorphous SiO_2 [10, 11]. Finally, the energetical and topological properties of the interstitial network for O_2 diffusion in amorphous SiO_2 were mapped onto lattice models and studied by means of Monte Carlo simulations. These simulations highlighted the percolative nature of the diffusion mechanism and yielded an effective activation energy in good agreement with experimental values [9].

In the thin-oxide regime, the diffusion rate in amorphous SiO_2 is expected to increase significantly because of the percolative nature of the diffusion mechanism [6, 7]. In fact, on a short-range scale, amorphous SiO_2 is not homogeneous and the diffusion rate increases due to the occurrence of small-barrier paths. In the following, we will specifically focus on this particular percolation effect. This effect should be contrasted with the presence of an oxide layer with a higher density in the neighbourhood of a silicon substrate, as revealed by x-ray reflectivity experiments [12, 13]. Indeed, this layer is expected to reduce the diffusivity [14]. The combined result of these two effects on the global diffusion rate has not so far been investigated within a realistic atomic-scale description. In particular, it is not clear whether the combined result would support the assumptions underlying current interpretations for the accelerated growth regime [8].

We are interested in understanding the behaviour of the O_2 diffusion coefficient in thin oxide films at Si–SiO_2 interfaces, as a function of oxide thickness. In order to address the thin-oxide regime, we will adopt an atomic-scale description along the lines developed in [9]. In this study, we assume that the migrating species which dominates the diffusion process is the interstitial O_2 molecule, although other mechanisms might be operative in the thin-oxide regime [15, 16]. In particular, we are interested in studying the interplay of two effects: the size effect resulting from the percolative nature of the diffusion paths and the occurrence of a dense SiO_2 layer at the interface.

Our paper is organized as follows. In section 2, we give a brief outline of the methodology used in this work. In section 3, we focus on the bulk structure of densified SiO_2 and obtain the corresponding potential energy landscape for O_2 diffusion. In section 4, we address the diffusion through thin oxide films at the Si–SiO_2 interface. Lattice models for oxide layers of various thicknesses and compositions are studied by means of Monte Carlo simulations.

2. Methods

The approach followed in the present work closely resembles the one in [9]. We here give a brief outline of the adopted methodologies. We first use a classical molecular dynamics scheme [17], with interatomic potentials for O–O, Si–O, and Si–Si pairs taken from [18], to generate a large set of model structures for densified SiO_2.

The interaction between the interstitial O_2 molecule and the SiO_2 network is also described by classical interatomic potentials. These potentials were derived in [9] from first principles. The latter classical potentials reproduce the first-principles interaction energies within an error of at most 0.2 eV [9].

Local minima for interstitial O_2 molecules were found by using a damped molecular dynamics scheme in which the intra-SiO_2 and O_2–SiO_2 interactions were combined. The initial positions of the O_2 were taken at random. For each model structure, this procedure was repeated until convergence was reached for the number of local minima.

We determined transition states between nearest-neighbour local minima by using a constrained molecular dynamics technique. For a pair of local minima A and B, the centre of mass of the O_2 molecule was continuously dragged from A to B across the SiO_2 network. At every step, the distance to B was successively reduced and kept fixed while the atomic positions of the entire system were allowed to relax fully. We used a step of 5×10^{-3} Å. The process associated with a given pair of minima was interrupted when the O_2 molecule encountered another local minimum during the evolution. The dragging approach used here was found to give the same results as the activation–relaxation technique (ART) [9, 19].

The classical scheme hence serves the following purposes:

(i) to construct model structures of densified amorphous SiO_2,

(ii) to determine the corresponding equilibrium sites for O_2,

(iii) to extract energy distributions of local minima and barriers for hopping between nearest-neighbour minima, and

(iv) to determine the connectivity of the interstitial network for oxygen diffusion on the basis of the location of the transition states.

To follow the diffusion process on larger spatial and temporal scales, it was necessary to resort to a simpler scheme. We therefore mapped the properties of the interstitial network for diffusion onto a lattice model for investigation by Monte Carlo simulation [9]. We adopted a normal lattice model whose sites and bonds were associated with local minima and transition states, respectively. Bonds were inserted between local minima in a statistical way, which preserved the local connectivity of the original atomic models. Diffusion events between nearest-neighbouring equilibrium sites for O_2 were described within the transition state theory [20]. According to this theory, the transition rates are determined by the relative energies of minima and saddle points [20]. We assumed unitary values for the attempt frequency and for the distance covered for transitions between neighbouring minima. These assumptions allowed us to obtain *relative* diffusion coefficients as a function of temperature or oxide thickness. Absolute diffusion coefficients depend on the choice for the attempt frequency and have not been extracted in this work.

We note that energy values corresponding to zero temperature were used in this paper as the diffusion mechanism for O_2 is dominated by energetic effects. For typical oxidation temperatures, entropic effects are estimated to be around 0.1 eV, which should be compared with the activation energy of about 1 eV.

Table 1. Comparison between the average structural parameters for amorphous SiO_2 (a-SiO_2) and densified amorphous SiO_2 (d-SiO_2), as obtained by means of classical molecular dynamics. The standard deviations are given after the ± sign.

	a-SiO_2	d-SiO_2
ρ (g cm^{-3})	2.2	2.4
Si–Si (Å)	3.12 ± 0.08	3.08 ± 0.12
Si–O (Å)	1.61 ± 0.02	1.61 ± 0.02
O–O (Å)	2.63 ± 0.09	2.63 ± 0.09
Si–O–Si (deg)	152 ± 12	149 ± 13
O–Si–O (deg)	109.4 ± 5.8	109.4 ± 5.8

3. O_2 diffusion in densified amorphous SiO_2

3.1. Model structures

We describe densified amorphous SiO_2 by a set of atomistic model structures, generated by classical molecular dynamics [17, 18]. We used periodically repeated cubic cells of fixed volume, corresponding to a density of 2.4 g cm^{-3}, as estimated from x-ray reflectivity measurements for the oxide in the vicinity of the Si–SiO_2 interface [12, 13]. Starting from random atomic positions, models of liquid SiO_2 were equilibrated at 3500 K for more than 300 ps. Amorphous structures were then obtained by quenching from the melt with a cooling rate of approximately 7 K ps^{-1} [17]. Full simulations lasted from 500 ps to 1 ns, depending on the size of the model structure. We constructed 16 model structures with the number of atoms in the periodic cell ranging between 72 and 90.

Each of the model structures consists of a random network of corner-sharing tetrahedral SiO_4 units, without any coordination defects. As compared with those of amorphous SiO_2 at the experimental density, structural parameters are only slightly affected by the increased density (table 1). The reduced volume per SiO_2 unit appears to be accommodated by the reduction of both the mean Si–O–Si bond angle and the Si–Si bond length. In addition, the calculated structure factor compares well with experimental data and correctly shows a shift of the first sharp diffraction peak towards a value of about 1.7 Å^{-1} [21]. This agreement indicates that the intermediate-range order in our model structures is properly described, despite their relatively small size.

3.2. Potential energy landscape

We first searched for equilibrium sites of interstitial O_2 molecules in densified amorphous SiO_2. We found a concentration of local minima of 6.7×10^{21} cm^{-3} and an average distance of about 5.3 Å between nearest-neighbour minima. These values differ only slightly from the case of amorphous SiO_2 at the normal density (5.4×10^{21} cm^{-3}, 5.7 Å) [9]. On the other hand, the energy distribution of local minima undergoes important changes. In particular, the mean value of this distribution shifts to a higher energy by 0.6 eV with respect to the mean value for amorphous SiO_2 at the normal density (figure 1) [9]. This property is consistent with the decrease of the average interstitial volume in densified amorphous SiO_2. In fact, the O_2-network energy was found to increase with decreasing interstitial volumes [9].

We then located the saddle points of the potential energy landscape and their corresponding energies. The transition states connect neighbouring minima by an asymmetric barrier. The energy barrier distribution associated with the low-barrier side is well described by a decaying exponential function with a decay constant of 1.72 eV. This should be compared with the

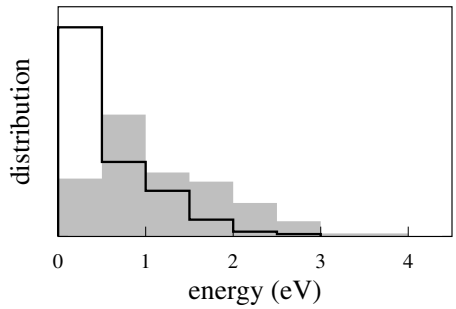

Figure 1. Comparison between the energy distributions of local minima for interstitial O_2 in densified amorphous SiO_2 (filled shaded histogram) and in amorphous SiO_2 at the normal density (open histogram).

corresponding value of 0.88 eV for amorphous SiO_2 at the normal density [9]. These results indicate that the potential energy landscape for O_2 diffusion in densified amorphous SiO_2 is considerably shifted towards higher energies as compared to amorphous SiO_2 at normal density.

As found from a statistical analysis of our atomistic model structures, the energy distributions of local minima and low-barrier-side transitions are uncorrelated. In fact, using the independence assumption, we were able to accurately reproduce the energy distributions of high-barrier-side transitions and saddle points.

The location of the transition states defines an interstitial network for O_2 diffusion. The local minima form the nodes of this network. Our analysis shows that in densified amorphous SiO_2 the number of connections per node can vary between 1 and 10. The average number of connections per node is found to be 4.1. The associated distribution can be well reproduced by a binomial distribution, characterized by parameters $n = 12$ and $p = 0.34$. This fact further supports the absence of correlations in the potential energy landscape for O_2 diffusion in densified amorphous SiO_2.

3.3. O_2 diffusion

To study the O_2 diffusion in densified amorphous SiO_2, we used a periodic fcc lattice model with $50 \times 50 \times 50$ independent sites. For a mean distance between local minima of 5.3 Å, this corresponds to a cubic volume of side $\sim$19 nm. Adopting the independence condition, we mapped the nearest-neighbour connectivity and the energy distributions derived from the atomistic structural models onto the lattice model. Monte Carlo simulations for 2000 diffusing particles were performed at temperatures ranging between 1000 and 1500 K [23], which are used in the technological process of oxidation. The minima and saddle points visited during the diffusion fell below the energies of competitive oxygen species [9], thereby indicating that the interstitial O_2 molecule also remains the favoured transported oxygen species in amorphous SiO_2 with a density of 2.4 g cm^{-3}. The calculated diffusion coefficients could be interpolated by means of an Arrhenius law. We found an effective activation energy of 2.0 eV, consistent with the experimental estimate of 2.0–2.4 eV for O_2 diffusion in an amorphous SiO_2 sample with a density of about 2.5 g cm^{-3} [14].

4. O_2 diffusion through the oxide layer at the Si–SiO_2 interface

4.1. Homogeneous oxide layer

To model the O_2 diffusion through oxide layers of different thicknesses, we performed Monte Carlo simulations on periodic lattice models with variable size in the direction z. In particular,

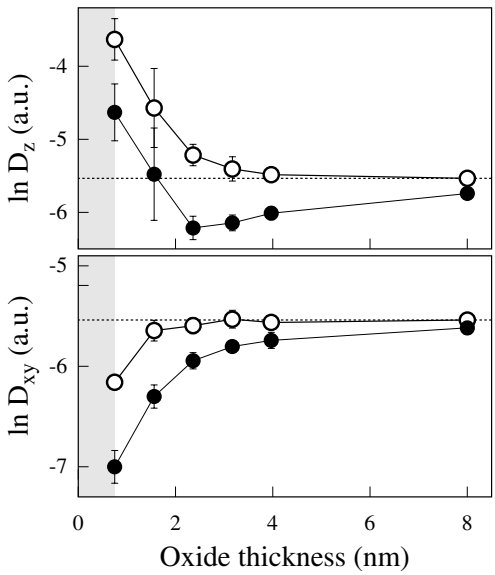

Figure 2. Calculated diffusion coefficients for homogeneous (open symbols) and nonhomogeneous (closed symbols) oxide layers of varying thickness at Si–SiO_2 interfaces. The upper (lower) panel shows the diffusion coefficient in a direction perpendicular (parallel) to the plane of the interface. The dotted line corresponds to the limit of bulk amorphous SiO_2 at normal density.

we considered fcc lattice models of $50 \times 50 \times N$ sites, where N was varied from 2 to 20, corresponding to oxide thicknesses between 1 and 10 nm. The reduced periodicity in the z-direction effectively models the diffusion in a thin oxide layer, as occurs at the Si–SiO_2 interface. In the other directions (x and y), the system is sufficiently large to recover the bulk limit. The diffusion coefficient was calculated at 1300 K, a temperature typically adopted for the thermal oxidation of silicon.

At first, we considered the case of homogeneous oxide layers. We assigned energies and connections to the lattice model according to distributions extracted for amorphous SiO_2 at normal density [9]. In particular, the correct nearest-neighbour connectivity on the fcc lattice could be obtained for a binomial function with $p = 0.27$. The results of the Monte Carlo simulations show that the rate for diffusion along z increases with decreasing oxide thickness (figure 2). This behaviour can be understood in terms of the percolative nature of the diffusion process. In fact, when the layer thickness drops, the number of low-barrier paths increases, resulting in an increase of the diffusion coefficient. For thick layers, the bulk value is recovered. We note that an increase of the diffusion coefficient for thin oxide layers *cannot* explain the anomalous deviations from the Deal–Grove model in the initial stages of oxidation [4, 8].

It is interesting to note that the behaviour of the diffusion coefficient in the xy-plane is very different, showing a decrease with decreasing oxide thickness. This behaviour corresponds to the gradual change of the diffusion coefficient when going from three to two dimensions. For example, the critical concentration of bonds for percolation increases from 0.24 to 0.50 when going from a three-dimensional cubic lattice to a two-dimensional square one [22].

4.2. Nonhomogeneous oxide layer

X-ray reflectivity experiments indicate the occurrence of a 10 Å thick oxide layer of higher density (2.4 g cm^{-3}) in the proximity of the Si–SiO_2 interface [12, 13]. We model the presence

of this dense layer by including in our lattice models two planes, on which we mapped the connectivity and energetic properties corresponding to amorphous SiO_2 with a density of 2.4 g cm^{-3} (section 3). For the remaining $N-2$ planes, we used the properties appropriate for amorphous SiO_2 at normal density [9]. The two layers are separated by two planes of interlayer connections. For one plane of such connections, we used the properties of amorphous SiO_2 and for the other those of densified SiO_2.

The diffusion coefficient for such oxide layers is given as a function of oxide thickness in figure 2. As expected, the diffusion coefficient is now lower than for homogeneous oxide layers. More interestingly, the diffusion coefficient falls below the bulk limit for oxide thicknesses larger than about 2 nm. This result indicates that the presence of a densified oxide can indeed account for a lower diffusion coefficient during oxidation. The diffusion coefficient is found to vary as a function of oxide thickness, approaching from below the bulk limit corresponding to amorphous SiO_2 at normal density. As long as the diffusion coefficient significantly differs from the bulk limit, deviations with respect to the Deal–Grove oxidation kinetics can be expected. This behaviour of the diffusion coefficient as a function of oxide thickness is in qualitative agreement with experimental data for the oxidation kinetics [5].

For oxide thicknesses below 2 nm, size effects due to percolation still dominate the diffusion coefficient in our model oxide layers. However, in these early stages of oxidation, other atomic-scale processes occur and might invalidate the underlying assumptions of our approach. Such processes include diffusion of peroxy linkages and charged species together with exchange processes between gas-phase and network oxygen atoms [15, 16].

For diffusion parallel to the plane of the interface, we found the same qualitative behaviour as for the homogeneous oxide. The presence of the dense oxide layer enhances the drop of the diffusion coefficient as the thickness decreases.

5. Conclusions

In the present paper, we present an atomic-scale investigation of the diffusion coefficient as a function of oxide thickness at Si–SiO_2 interfaces. For homogeneous oxide layers, we first found that the diffusion coefficient increases with decreasing oxide thickness, because of percolation effects. This behaviour appears to be inconsistent with experimental data for the oxidation kinetics [5] which instead indicates a decrease of the diffusion rate for oxide thicknesses below 20 nm.

We then modelled the structural properties of the oxide layer accounting for a thin densified oxide layer in the vicinity of the silicon substrate. The thickness and the density of this layer were taken from x-ray reflectivity measurements [12, 13]. The presence of such a layer strongly affects the diffusion coefficient, which is found to drop below the bulk SiO_2 value for thicknesses larger than 2 nm. This behaviour is consistent with experimental data for the oxidation kinetics [5].

Acknowledgments

We acknowledge support from the Swiss National Science Foundation (grant Nos 21-55450.98 and 620-57850.99) and the Swiss Centre for Scientific Computing.

References

[1] Green M L, Gusev E P, Degraeve R and Garfunkel E L 2001 *J. Appl. Phys.* **90** 2057
[2] Deal B E and Grove A S 1965 *J. Appl. Phys.* **36** 3770

[3] Fargeix A, Ghibaudo G and Kamarinos G 1983 *J. Appl. Phys.* **54** 2878
[4] Mott N F, Rigo S, Rochet F and Stoneham A M 1989 *Phil. Mag.* B **60** 189
[5] Massoud H Z, Plummer J D and Irene E A 1985 *J. Electrochem. Soc.* **132** 1745
[6] Verdi L, Miotello A and Kelly R 1994 *Thin Solid Films* **241** 383
[7] Verdi L and Miotello A 1995 *Phys. Rev.* B **51** 5469
[8] de Almeida R M C, Gonçalves S, Baumvol I J R and Stedile F C 2000 *Phys. Rev.* B **61** 12992
[9] Bongiorno A and Pasquarello A 2002 *Phys. Rev. Lett.* **88** 125901
[10] Rosencher E, Straboni A, Rigo S and Amsel G 1979 *Appl. Phys. Lett.* **34** 254
[11] Norton F J 1961 *Nature* **191** 701
[12] Awaji N, Ohkubo S, Nakanishi T, Sugita Y, Takasaki K and Komiya S 1996 *Japan. J. Appl. Phys.* **35** L67
[13] Kosowsky S D, Pershan P S, Krish P S, Bevk J, Green M L, Brasen D, Feldman L C and Roy P K 1997 *Appl. Phys. Lett.* **70** 3119
[14] Devine R A B, Capponi J J and Arndt J 1987 *Phys. Rev.* B **35** 770
[15] Ganem J-J, Trimaille I, André P, Rigo S, Stedile F C and Baumvol J R 1997 *J. Appl. Phys.* **81** 8109
[16] Stoneham A M, Szymanski M A and Shluger A L 2001 *Phys. Rev.* B **63** R241304
[17] Vollmayr K, Kob W and Binder K 1996 *Phys. Rev.* B **54** 15808
[18] van Beest B W H, Kramer G J and van Santen R A 1990 *Phys. Rev. Lett.* **64** 1955
[19] Barkema G T and Mousseau N 1996 *Phys. Rev. Lett.* **77** 4358
[20] Vineyard G H 1957 *J. Phys. Chem. Solids* **3** 121
[21] Inamura Y, Arai M, Kitamura N, Bennington S M and Hannon A C 1998 *Physica* B **241** 903
[22] Stauffer D 1985 *Introduction to Percolation Theory* (London: Taylor and Francis)
[23] Roling B 2000 *Phys. Rev.* B **61** 5993